Structure-Dynamics-Function Relationships in Asian Elephant (*Elephas maximus*) Myoglobin. An Optical Spectroscopy and Flash Photolysis Study on Functionally Important Motions

Antonio Cupane,* Maurizio Leone,* Eugenio Vitrano,* Lorenzo Cordone,* Urs R. Hiltpold,‡ Kaspar H. Winterhalter,‡ Weiming Yu,‡ and Ernesto E. Di Iorio‡

*Istituto di Fisica, Università di Palermo, Palermo, Italy, and ‡Laboratorium für Biochemie I, Eidgenössische Technische Hochschule, Zurich, Switzerland

ABSTRACT In this work we report the thermal behavior (10–300 K) of the Soret band lineshape of deoxy and carbonmonoxy derivatives of Asian elephant (*Elephas maximus*) and horse myoglobins together with their carbon monoxide recombination kinetics after flash photolysis; the results are compared to analogous data relative to sperm whale myoglobin.

The Soret band profile is modeled as a Voigt function that accounts for the coupling with high and low frequency vibrational modes, while inhomogeneous broadening is taken into account with suitable distributions of purely electronic transition frequencies. This analysis makes it possible to isolate the various contributions to the overall lineshape that, in turn, give information on structural and dynamic properties of the systems studied. The optical spectroscopy data point out sizable differences between elephant myoglobin on one hand and horse and sperm whale myoglobins on the other. These differences, more pronounced in deoxy derivatives, involve both the structure and dynamics of the heme pocket; in particular, elephant myoglobin appears to be characterized by larger anharmonic contributions to soft modes than the other two proteins.

Flash photolysis data are analyzed as sums of kinetic processes with temperature-dependent fractional amplitudes, characterized by discrete pre-exponentials and either discrete or distributed activation enthalpies. In the whole temperature range investigated the behavior of elephant myoglobin appears to be more complex than that of horse and sperm whale myoglobins, which is in agreement with the increased anharmonic contributions to soft modes found in the former protein. Thus, to satisfactorily fit the time courses for CO recombination to elephant myoglobin five distinct processes are needed, only one of which is populated over the whole temperature range investigated.

The remarkable convergence and complementarity between optical spectroscopy and flash photolysis data confirms the utility of combining these two experimental techniques in order to gain new and deeper insights into the functional relevance of protein fluctuations.

INTRODUCTION

The structure and, in more recent years, the dynamics of the heme pocket distal side are thought to play an important role in regulating the functional properties of heme proteins (Braunstein et al., 1988; Di Iorio et al., 1987; Mims et al., 1983). In comparative studies on heme proteins, sperm whale myoglobin (Sw-Mb), the most studied and possibly best known protein, is usually taken as the reference, and the role of distal residues is investigated by examining both naturally occurring and, more recently, recombinant mutants. The choice of Sw-Mb as a reference is unquestionably related to its high availability (at least until recently). However, from a structural point of view there is no reason why Sw-Mb should be taken as reference; to the contrary, a comparison with other 61 myoglobins shows for instance that (*a*) at position 45 (CD3) all myoglobins have a lysine, the only exceptions being sperm whale and aardvark Mb, where it is replaced by an arginine; (*b*) Gly15 (A13) is replaced by an alanine only in the myoglobins from some whales and from map and green sea turtle or by threonine in American alligator Mb; (*c*) Gly35 (B16), present in most myoglobins, is substituted by a serine, the same replacement occurring only in grey and harbor seals (W. Yu and E. E. Di Iorio, unpublished results). No comparative data are available which prove that the structural differences between Sw-Mb and the other myoglobins have functional implications, but we consider it a safe policy to use horse Mb (Ho-Mb), in addition to Sw-Mb, as a reference.

Elephant myoglobin (El-Mb) is particularly interesting for investigations on distal side effects since in position 64 (E7) carries a glutamine instead of the highly conserved histidine. In addition to this important replacement, El-Mb displays 27 and 21 additional substitutions compared to Sw-Mb and to Ho-Mb, respectively, only two of which are nonconservative. Thus El-Mb has a threonine at position 13 (A11) replacing either a valine, an isoleucine, or an alanine present in the other myoglobins, and a phenylalanine as residue 27 (B8) instead of a glutamic acid (in ~70% of the other myoglobins including also Ho-Mb) or an aspartic acid (in the remaining myoglobins including Sw-Mb). Compared to Sw-Mb, El-Mb is characterized by a markedly reduced autooxidation rate (Romero-Herrera et al., 1981), an increased

Received for publication 28 June 1993 and in final form 28 June 1993.

Address reprint requests to Dr. Lorenzo Cordone, Istituto di Fisica dell'Università Degli Studi, Via Archirafi 36, I-90123 Palermo, Italy.

0006-3495/93/12/2461/12 $2.00

redox potential (Bartnicki et al., 1983), and a decreased CO dissociation rate, the association constant being practically unchanged (Romero-Herrera et al., 1981). The structure at the distal side of the heme pocket of El-Mb has been investigated by two-dimensional NMR spectroscopy (Yu et al., 1990; Vyas et al., 1993) and by resonance Raman (RR) spectroscopy (Kerr et al., 1985). The former investigation indicates the presence of a phenylalanine in the heme pocket of El-Mb located where a cavity is found in Sw-Mb and interacting with the bound ligand; this leads to a crevice that is both more crowded and hydrophobic than in Sw-Mb. Moreover, hydrogen bonding of the glutamine N_ϵ proton to the iron-bound ligand is present in cyano-met El-Mb, in analogy with that formed by the distal histidine N_ϵ proton in Sw-Mb (Vyas et al., 1993). On the other hand, RR spectra of carbonyl El-Mb show that the bound CO molecule is tilted off the heme normal at least as much as in Sw-Mb (Kerr et al., 1985). The peculiar functional properties of El-Mb mentioned above can all be rationalized in terms of steric and hydrophobic effects at the heme pocket.

The particular structural situation proposed by Yu et al. (1990) for the heme pocket of El-Mb renders this protein particularly well suited for investigations on the interplay between protein dynamics and steric phenomena.

Optical spectroscopy over broad temperature ranges (20–300 K) have proved to be very useful for investigating the stereodynamic properties of heme proteins (Cordone et al., 1986; Cupane et al., 1988; Leone et al., 1987, 1992; Di Iorio et al., 1991). In particular, for the Soret band of heme proteins a nonheuristic deconvolution of the measured spectra is possible, and the various contributions to the overall bandwidth can be singled out (Di Pace et al., 1992; Cupane et al., 1993). Furthermore, the temperature dependence of the spectra provides information on the relative importance of the various mechanisms involved in determining the spectral line shapes, including homogeneous broadening due to nonradiative decay of the excited electronic state, coupling with high-frequency nuclear vibrations (responsible for the vibronic structure of the spectra), gaussian broadening due to the coupling with a bath of low frequency motions, and inhomogeneous broadening due to conformational heterogeneity. The thermal evolution of the Soret band, therefore, provides information on the stereodynamic properties of the molecule under investigation. On the other hand, flash photolysis measurements on heme proteins, carried over broad temperature ranges, allow for direct investigations of the interplay between dynamics and function (Austin et al., 1975; Steinbach et al., 1991). This experimental approach has provided the first evidence for structural heterogeneity in proteins, as a consequence of fluctuations (Austin et al., 1975).

The combination of optical spectroscopy and flash photolysis for studies of protein dynamics has already proved very useful (Di Iorio et al., 1991). In this work we apply the two approaches to El-Mb, using Sw-Mb and Ho-Mb as references, and try to gain information on the effect of structural alterations within the heme pocket on the interplay between protein dynamics and function.

MATERIALS AND METHODS

Samples

Sw-Mb and Ho-Mb were purchased from Sigma Chemical Co. (St. Louis, MO) and used without further purification. Stock solutions ($\sim 6 \times 10^{-4}$ M) of these proteins were prepared immediately before use by dissolving an appropriate amount of the lyophilized commercial product in 0.1 M phosphate buffer (pH 7.0). The resulting met-Mb solution was centrifuged to remove any precipitate. Glycerol (Fluka, Buchs, Switzerland) and all other chemicals were analytical grade and used without further purification. El-Mb was prepared as a carbonyl derivative following a modification of a previously described method (Wittenberg and Wittenberg, 1981). Elephant skeletal muscle (~200 g) was washed with 20 mM Tris/HCl buffer (pH 8.4) containing 1 mM EDTA and homogenized with a Warren blender in four volumes of the same buffer saturated with CO. The homogenate was spun for 10 min at $\sim 10{,}000 \times g$ and ammonium sulfate was added to the supernatant, at 0°C and under continous stirring, up to 65% saturation. The solution was kept above pH 8 by the addition of ammonium hydroxide. After equilibration for 1 h, the precipitate was separated by centrifugation and the supernatant was dialyzed against 20 mM Tris/HCl pH 8.4, containing 1 mM EDTA. The resulting solution was concentrated by ultrafiltration under 300–400 kPa of CO to a final volume of ~10 ml before being applied on a Sephadex G-100 (ϕ 3.5 × 40 cm) equilibrated and eluted with the above Tris-HCl buffer. The El-Mb containing fractions were pooled, concentrated again to ~10 ml, and applied on a DEAE Sephacell column (ϕ 2.5 × 30 cm) equilibrated and eluted with the same Tris-HCl buffer. The fractions containing only El-Mb, as judged from polyacrylamide gel electrophoresis carried out under denaturating and nondenaturating conditions, were concentrated to ~6 mM and stored under liquid nitrogen in small aliquots to be thawed immediately before use. For the conversion of the protein to the oxy derivative the protein was exposed to intense illumination under a flux of pure oxygen, as previously described (Di Iorio, 1981).

Optical spectroscopy

For spectrophotometric measurements on the carbonyl derivatives, the Mb stock solution was carefully saturated with CO and subsequently treated with dithionite under strictly anaerobic conditions. The resulting solution was immediately diluted with water-cosolvent-buffer mixtures, also saturated with CO, to a final composition of 0.1 M phosphate (pH 7 in water at room temperature), 65% v/v glycerol, $\sim 6 \times 10^{-6}$ M protein and $\sim 3 \times 10^{-4}$ M dithionite. Preparation of the deoxy-Mb samples was done by thorough deoxygenation in a tonometer of ~10 ml of a solution containing 0.1 M phosphate (pH 7) in water at room temperature, 65% v/v glycerol, and $\sim 10^{-5}$ M Mb, followed by the addition of 50 μl of a 2% dithionite solution, prepared under strictly anaerobic conditions. Immediately after preparation the sample, in the carbonyl or deoxy form, was transferred anaerobically to a metacrylate cell (UV grade; Kartell, Milano, Italy) with a 1-cm path length mounted in the cryostat.

Spectra in the 500–350 nm region were recorded in digital form at 0.4-nm intervals with a Jasco Uvidec 650 spectrophotometer (Japan Spectroscopic Co., Tokyo) set at a 0.4-nm bandwidth, a time constant of 1 s, and a scan speed of 40 nm/min. All other experimental details were as previously described (Cordone et al., 1986). We stress that our samples remained homogeneous and transparent at all temperatures; the absence of light scattering due to sample cracking results in a remarkable stability of the baseline with temperature and allows the data analysis described later.

The baseline, recorded at room temperature with the same cuvette used for the measurements and filled with the water-cosolvent-buffer mixture used for diluting the protein under investigation, was subtracted from each spectrum. At the concentrations used, light absorption due to dithionite

becomes relevant below ~370 nm. For this reason the spectral analysis was limited to the region between 500 and 380 nm. Spectral deconvolutions were performed on a Microway I860 add-on board for IBM-PC (Microway Europe, Ltd., Kingston upon Thames, England), using a Marquardt-type (Marquardt, 1963) nonlinear least-squares algorithm. The 67% confidence limits on the fitted parameters were calculated by inversion of the curvature matrix (Bevington, 1969, pp. 242–245), within the approximation of a parabolic χ^2 hypersurface around the minimum.

To isolate the Soret band from the background generated by other electronic transitions, the absorbance at 490 nm was brought to a common value (0 and 0.02, respectively, for the CO and deoxy derivatives) for all the spectra and a gaussian component, centered at 29,000 cm^{-1} for the carbonyl and at 27,000 cm^{-1} for the deoxy samples, was included in the analysis to account for contributions due to the N band.

An analytical expression for the Soret band profile at various temperatures is obtained by considering a single electronic transition coupled with several harmonic, Franck-Condon active, vibrational modes and treating the system within the Born-Oppenheimer and Condon approximations. Details on the theoretical approach used have been given in previous publications (Di Pace et al., 1992; Cupane et al., 1993). Here we report only a short summary.

It has been shown that absorbance at frequency ν can be written as a Voigtian (i.e., a gaussian convolution of lorentzians):

$$A(\nu) = M\nu \sum_{m_1,\ldots,m_{N_h}}^{\infty} \prod_{i}^{N_h} \frac{S_i^{m_i} e^{-S_i}}{m_i!} \times \frac{\Gamma}{[\nu - \nu_0 - \sum_i^{N_h} m_i R_i \nu_i(g)]^2 + \Gamma^2} \otimes \frac{1}{\sigma} e^{-\nu^2/2\sigma^2} \quad (1)$$

where M is a constant proportional to the square of the electric dipole moment, Γ is a damping factor related to the finite lifetime of the excited state (homogeneous broadening), the product extends to all high-frequency vibrational modes (i.e., with $h\nu_i \gg k_B T$) coupled to the electronic transition, the summations to their occupation numbers, ν_i, S_i, and R_i, are, respectively, the frequency, linear, and quadratic coupling constants for the ith high frequency mode, and ν_0 can be safely assumed, for the Soret band, to be the peak frequency. The symbol $\otimes$ indicates the convolution operator. Coupling of the electronic transition with low-frequency modes (i.e., with frequency smaller than the observed bandwidth) is treated within the "short times approximation" (Chan and Page, 1983); this brings about the convolution with a gaussian lineshape and contributes the temperature-dependent terms $\sigma^2(T)$ and $\nu_0(T)$ (see Eqs. 4 and 5 below), respectively, to the linewidth and peak position of the band.

Further contributions to the spectral linewidth are given by inhomogeneous broadening effects arising from different conformational substates and heme environments (Frauenfelder et al., 1988). For the ligated derivatives, due to the in-plane position of the iron atom, inhomogeneous broadening contributions can be modeled as a gaussian distribution of purely electronic transitions (ν_{00}), thus contributing an additional term (σ_{in}) to the width of the gaussian component of the Voigtian in Eq. 1. For the deoxy derivative, it has been suggested (Srajer et al., 1986; Srajer and Champion, 1991) that the energy of the $\pi \rightarrow \pi^*$ electronic transition responsible for the Soret band depends upon the position of the iron atom relative to the heme plane, and therefore

$$\nu_{00} = \nu_{00}(Q = 0) + aQ + bQ^2 \quad (2)$$

where Q is a generalized iron coordinate representing both the out-of-plane displacement and other angular coordinates, and a and b are parameters that reflect the electronic properties of the iron-porphyrin system. Usually only the quadratic dependence is considered and the linear term in Eq. 2 is neglected (Srajer et al., 1986; Srajer and Champion, 1991; Cupane et al., 1993). The coordinate Q is assumed to have a statistical distribution of width δ around the mean coordinate position Q_0 that brings about a nongaussian distribution of transition frequencies. The resulting analytical expression, which suitably describes the Soret band lineshape for the deoxy derivatives, is

$$A(\nu) = V(\nu) \otimes \frac{1}{2\delta\sqrt{(\nu - \nu_0)2\pi b}} \left[\exp\left(- \frac{[(\nu - \nu_0)^{1/2} + Q_0\sqrt{b}]^2}{2b\delta^2} \right) + \exp\left(- \frac{[(\nu - \nu_0)^{1/2} - Q_0\sqrt{b}]^2}{2b\delta^2} \right) \right] \quad (3)$$

where $V(\nu)$ is given by Eq. 1.

The analysis of the Soret absorption spectra of ligated and deoxy derivatives is based on fittings of the experimental data to Eqs. 1 and 3, respectively. Details on the numerical calculations have been given in previous publications (Di Pace et al., 1992; Cupane et al., 1993). The fitting parameters are M, Γ, S_i, σ, ν_0, and, only for the deoxy derivatives, $Q_0\sqrt{b}$ and $\delta\sqrt{b}$. ν_i values relative to high frequency modes are taken from resonance Raman (RR) spectra reported in the literature (Tsubaki et al., 1982; Kerr et al., 1985; Asher et al., 1981; Bangcharoenpaurpong et al., 1984). The most coupled modes are those centered at 350, 676, 1100, and 1374 cm^{-1} for CO derivatives and 370, 674, and 1357 cm^{-1} for the deoxy, whereas other less coupled modes do not contribute significantly to the lineshapes and are therefore neglected. It is worth mentioning that in RR spectra of heme proteins 676 cm^{-1} and 1375 cm^{-1} for the CO derivatives, and, respectively, 674 cm^{-1} and 1357 cm^{-1} for the deoxy, correspond to very sharp lines and are thought to arise from in-plane vibrational modes of the heme group, that is, $\nu_7 \equiv \delta C_a C_b N$ and $\nu_4 \equiv \delta C_a N$, respectively (Spiro, 1983). On the contrary, 350 cm^{-1} (or 370 cm^{-1}) and 1100 cm^{-1} are "average effective" frequencies accounting for several quasi-degenerate peaks. Both in-plane and out-of-plane modes contribute to these spectral regions. For deoxy derivatives we also attempted to include in the fittings coupling to the 1100 cm^{-1} mode, but the resulting linear coupling strength turned out to be smaller than 0.01. At low temperatures, S_i values are rather well determined in view of the clear vibronic structure of the band (see Fig. 2); therefore, to avoid fitting ambiguities arising from line broadening and consequent difficulties in resolving the high-temperature vibronic structure, parameters S_i were determined from the low-temperature spectra and kept fixed at such values in the analysis of the spectra recorded at high temperatures. Temperature-independent S_i values are in agreement with previous reports (Di Pace et al., 1992; Cupane et al., 1993; Schomacker and Champion, 1989). R_i were assumed to be ~1.

Within the harmonic approximation and considering the coupling of the Soret band with a "bath" of low-frequency modes, the temperature dependence of the parameters σ^2 and ν_0 in Eqs. 1 and 3 can be expressed as

$$\sigma^2 = NSR^2\langle\nu\rangle^2 \coth(h\langle\nu\rangle/2kT) + \sigma_{in}^2 \quad (4)$$

$$\nu_0 = \nu_{00} - \tfrac{1}{4}N\langle\nu\rangle(1 - R)\coth(h\langle\nu\rangle/2kT) + C \quad (5)$$

where $\langle\nu\rangle$, S, and R are the effective frequency, linear, and quadratic coupling constants of the low-frequency bath, N is the number of soft modes, ν_{00} is the frequency of the purely electronic (0–0) transition, and C takes into account other temperature-independent contributions to the peak position of the band. As already discussed, the term σ_{in}^2 in Eq. 4 was used only in the case of CO derivatives since for the deoxy spectra the effect of inhomogeneous broadening is taken into account by the parameter $\delta\sqrt{b}$.

Flash photolysis

The samples were prepared for flash photolysis measurements and data were collected and averaged as previously described (Di Iorio et al., 1991, 1993; Richter and Di Iorio, 1991). Final concentrations in the samples were: 0.1 M phosphate (pH 7 in water at room temperature), 75% v/v glycerol, and ~10^{-4} M Mb; trace amounts of dithionite were also present, and the solutions were saturated with pure CO at room temperature. Details on the iterative global least-squares procedure used for the analysis of the data and for the determination of the 67% confidence limits on the fitted parameters are given elsewhere (Di Iorio et al., 1991, and references therein). The models used for the fittings were always a sum of processes with discrete

pre-exponentials and either discrete or distributed activation enthalpies. The total number of processes and the use of a discrete or distributed activation enthalpy model was decided on the basis of an F-test (Bevington, 1969, pp. 195–202). Following this strategy, traces recorded between 40 K and 210 K have been analyzed using the sum of three kinetic processes, each characterized by distinct distributions of activation enthalpy and discrete preexponentials. The absorbance change relative to trace j at time t and temperature T_j was thus defined as

$$\Delta A_j(t) = \Delta A_{\text{total}_j} \sum_i f_{i,j} \cdot \int_0^\infty dH \cdot g_{i,j}(H) \cdot \exp\left[- k_{0_{i,j}} \cdot \exp\left(- \frac{H}{RT_j} \right) \cdot t \right] \quad (6)$$

with the condition that the sum of the fractions $f_{i,j}$ is 1. The parameterization of the enthalpy distribution, which represents the probability of finding the protein in a conformational substate characterized by an activation enthalpy between H and $H + dH$, was done using the following modification of the Young and Bowne (1985) model:

$$g_{i,j}(H) = H^{H_{\text{peak}_{i,j}} \cdot \psi_{i,j}} \cdot \exp(-\psi_{i,j} \cdot H) \quad (7)$$

normalized to unity area.

Therefore, the parameters to be determined for each component i and trace j were the time zero amplitude $\Delta A_{\text{total}\ j}$, the fractions $f_{i,j}$, the pre-exponentials $k_{0i,j}$, $H_{\text{peak}\ i,j}$, and $\Psi_{i,j}$. Whenever any of the parameters did not appreciably change from trace to trace they were assumed to have the same value for the whole set of data being analyzed and were treated as a single variable. As an example, each of the three kinetic processes used to approximate the data recorded in the 40–110 K and in the 120–180 K ranges was considered to have temperature-independent ΔA_{total}, k_0, H_{peak}, and Ψ, while the fractions f were left free to vary for each component i and trace j.

Data collected between 220 K and 230 K were analyzed using a sum of two distributed and one exponential process, and those referring to the 240–280 K range were treated as sum of one distributed and two discrete processes. Only traces recorded at 290 K and 300 K have been analyzed in terms of a sum of two components, one distributed and one discrete.

EPR spectroscopy

For the EPR (electron paramagnetic resonance) measurements nitrosyl Mb was prepared by treatment with nitrite and ascorbate (Trittelvitz et al., 1975). For this purpose 100 μl of a ~4 mM stock solution of carbonyl El-Mb, in 20 mM phosphate (pH 7), were extensively purged with nitrogen before being treated with 8 μl of 2.5 M sodium ascorbate and 20 μl of 2.5 M sodium nitrite (both titrated to pH 7) and mixed with 72 μl of 0.55 M citrate buffer. The solution was then transferred to the EPR tube and immediately frozen in liquid nitrogen. The pH of the solutions was measured at the end of the measurements. EPR spectra were recorded on a Bruker ESP 300 spectrometer equipped with a helium cooling system from Air Products. Standard mode first-derivative spectra were taken at 77 K with 100 MHz field modulation. For resolution enhancement, the second derivatives have been computed from the digitized experimental spectra.

RESULTS AND DISCUSSION

Optical spectroscopy

Fig. 1 shows the 20 K spectra of carbonyl and deoxy El-Mb together with the profiles obtained from their analysis in terms of Eqs. 1 and 3, respectively. Analogous data on Ho-Mb (data not shown) display features very similar to those reported in previous publications for Sw-Mb (Di Pace et al., 1992; Cupane et al., 1993). The values of the linear coupling constants for the high-frequency modes and of the lorentzian width Γ, obtained from fittings of the spectra of the three proteins to Eqs. 1 and 3, are reported in Table 1.

Interesting information can already be obtained from this first set of data; indeed, although the linear coupling constants S_i relative to El-Mb-CO compare quite well with those relative to Ho-Mb-CO and Sw-Mb-CO, sizable differences are found for the deoxy derivatives (see Table 1). Thus, for El-Mb the linear coupling constants for the 370 and 1357 cm^{-1} modes are considerably smaller than those observed in Sw-Mb and Ho-Mb, whereas for the 674 cm^{-1} mode S_i is larger. Considering that the Soret band arises from a $\pi \rightarrow \pi^*$ electronic transition within the heme ring and that the heme is planar in CO derivatives while being domed in the deoxy derivatives, we suggest that this feature arises from differences in heme doming between El-Mb and Sw or Ho-Mb; plausibly, this is related to the crowding of the El-Mb heme pocket observed by NMR spectroscopy (Yu et al., 1990; Vyas et al., 1993) and described in the introduction. Moreover, the reduced intensity of the peaks in the 300–400 cm^{-1} region of the RR spectra of El-Mb compared with Sw-Mb (Kerr et al., 1985) agrees with the smaller S_{370} value obtained in this work. In spite of the fact that the low temperature values of Γ are the same for the three proteins and equally influenced by changes in the ligation state (Table 1), the abrupt change of Γ reported by Di Pace et al. (1992) for Sw-Mb-CO at the solvent glass transition (~180 K) is also observed for Ho-Mb-CO but not for El-Mb-CO (data not shown). This is plausibly related to peculiar structural features of the heme pocket in El-Mb: indeed, an increased crowding of the distal heme pocket in El-Mb could prevent (or at least greatly hinder) a change in the tilting of the bound CO molecule relative to the heme normal, which has been suggested to be responsible for the Γ change observed in Sw-Mb-CO (Di Pace et al., 1992). It is worth mentioning that large uncertainties in the estimates of Γ and of S_i can be excluded in view of the almost lorentzian shape displayed by the red edge of the Soret band and of its clear vibronic structure at low temperatures. This is shown in Fig. 2, where we compare the 20 K spectra of the deoxy derivatives of El-Mb, Ho-Mb, and Sw-Mb after subtraction of the N band and suitable peak frequency shift; it is unequivocal that the red edge shape is the same in the three spectra (leading to equal values of Γ), whereas the coupling with the 674 cm^{-1} mode is sizably larger for El-Mb than for Ho-Mb and Sw-Mb.

The temperature dependence of ν_0 and σ^2 is depicted in Figs. 3 and 4. For the three proteins, Eqs. 4 and 5 cannot describe the temperature dependence of these two parameters in the whole 20–300 K range. This fact is obvious for ν_0 (see Fig. 3). For the particular case of σ^2 (Fig. 4) we wish to emphasize that, for $T \rightarrow \infty$, Eq. 4 becomes a straight line whose intercept at $T = 0$ gives σ^2_{in}, while the straight line tangent to the high-temperature experimental points extrapolates at $T = 0$ to physically meaningless negative σ^2_{in} values. A proper fitting of the thermal behavior of ν_0 and σ^2 to Eqs. 4 and 5, respectively, can only be performed in the range

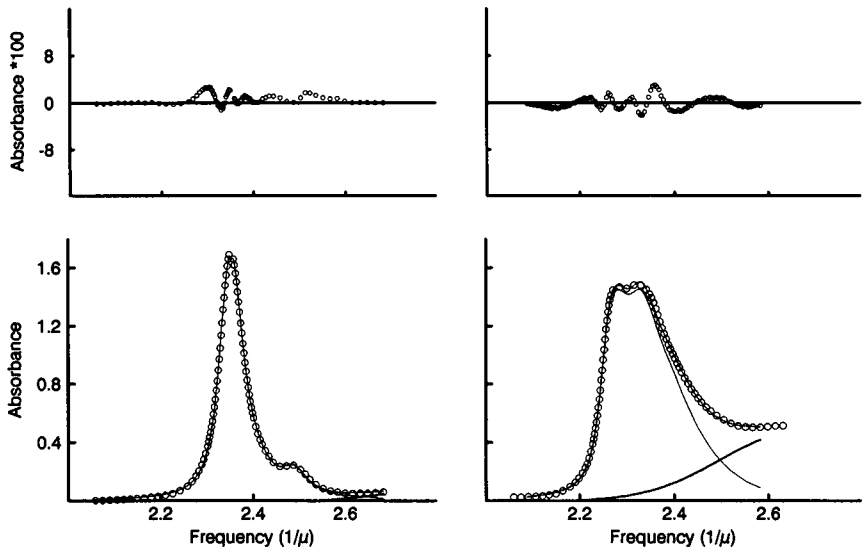

FIGURE 1 Spectra of El-Mb-CO (*left*) and El-Mb (*right*) at 20 K. Circles represent the experimental points and the continuous lines the fittings in terms of Eqs. 1 and 3 respectively as well as contributions from the N band and from the "naked" Soret band. For the sake of clarity not all experimental points have been reported. The residuals between the experimental and fitted spectra are given in the upper panels on an expanded scale.

TABLE 1 Low-temperature (T = 20 K) linear coupling constants of the high-frequency modes and Γ values for the proteins investigated

	S_{370}	S_{674}	S_{1100}	S_{1357}	Γ/cm^{-1}
El-Mb	<0.01	0.34 ± 0.02	<0.01	<0.01	170 ± 8
Ho-Mb	0.36 ± 0.03	0.25 ± 0.02	<0.01	0.10 ± 0.01	170 ± 10
Sw-Mb	0.32 ± 0.02	0.24 ± 0.02	<0.01	0.10 ± 0.01	180 ± 10
	S_{350}	S_{676}	S_{1100}	S_{1374}	Γ/cm^{-1}
El-MbCO	0.09 ± 0.01	0.05 ± 0.01	0.01 ± 0.005	0.09 ± 0.01	210 ± 10
Ho-MbCO	0.10 ± 0.01	0.06 ± 0.01	0.02 ± 0.005	0.09 ± 0.01	213 ± 8
Sw-MbCO	0.12 ± 0.02	0.06 ± 0.01	0.02 ± 0.008	0.09 ± 0.01	211 ± 7

20–160 K for the CO derivatives and in the range 20–110 K for the deoxy derivatives. The continuous lines in Figs. 3 and 4 refer to such fittings, and the corresponding values of the parameters are reported in Table 2. The above finding indicates that for the three proteins investigated and in both ligation states there is a sizable coupling of the $\pi \rightarrow \pi^*$ transition responsible for the Soret band with a bath of low-frequency modes characterized, in the three proteins, by similar mean effective frequencies as well as linear and quadratic coupling constants. The results of this analysis show that the low temperature values of ν_0 (Fig. 3) or, equivalently, of $\nu_{00} + C$ (Table 2), are smaller for El-Mb than for Sw-Mb and Ho-Mb, irrespective of the ligation state. This finding confirms the peculiar electronic properties of the iron-porphyrin system in El-Mb as compared to the other two myoglobins. The deviations of σ^2 from the behavior predicted by Eq. 4 occurring at high temperatures are evident in Fig. 4 for the three proteins; such deviations have been attributed to anharmonicity in nuclear motions (Di Pace et al., 1992). A peculiar increase of the average atomic fluctuations, occurring at temperatures higher than ~180 K, emerges from several investigations on a number of different proteins, based on independent experimental and computational approaches (Doster et al., 1989; Krupianskii et al., 1990; Loncharich and Brooks, 1990; Parak, 1989; Smith et al., 1990; Winkler et al., 1990) and has been attributed to a transition in protein mobility from a low-temperature behavior characterized by essentially harmonic oscillations of the nuclei around their equilibrium positions to a high-temperature

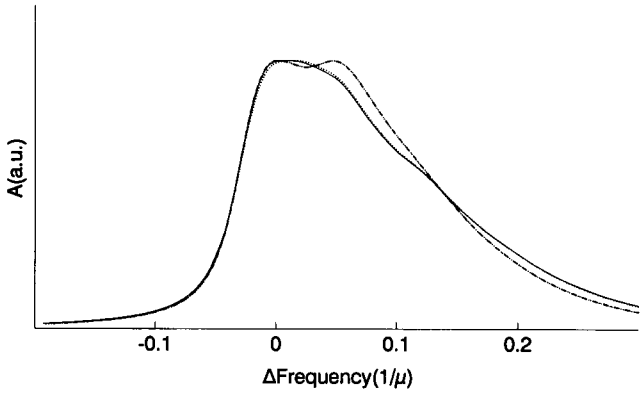

FIGURE 2 Soret band of Sw-Mb (*continuous line*), Ho-Mb (*dotted line*), and El-Mb (*dashed line*) at 20 K. The profiles have been obtained from the experimental spectra by subtraction of the N band, suitable shift along the frequency axis and intensity normalization.

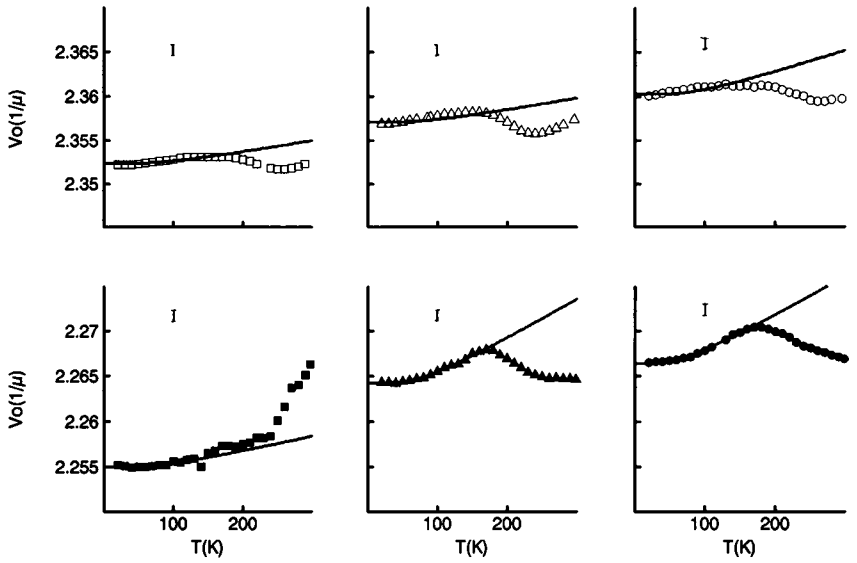

FIGURE 3 Temperature dependence of ν_0 values relative to elephant (*left panels; squares*), horse (*center panels; triangles*), and sperm whale myoglobin (*right panels; circles*). Open symbols and upper panels refer to CO derivatives, full symbols and lower panels to deoxy ones. The continuous lines represent fittings of the data in the temperature range 20–160 K (CO derivatives) and 20–110 K (deoxy derivatives) in terms of Eq.5. Typical error bars are reported.

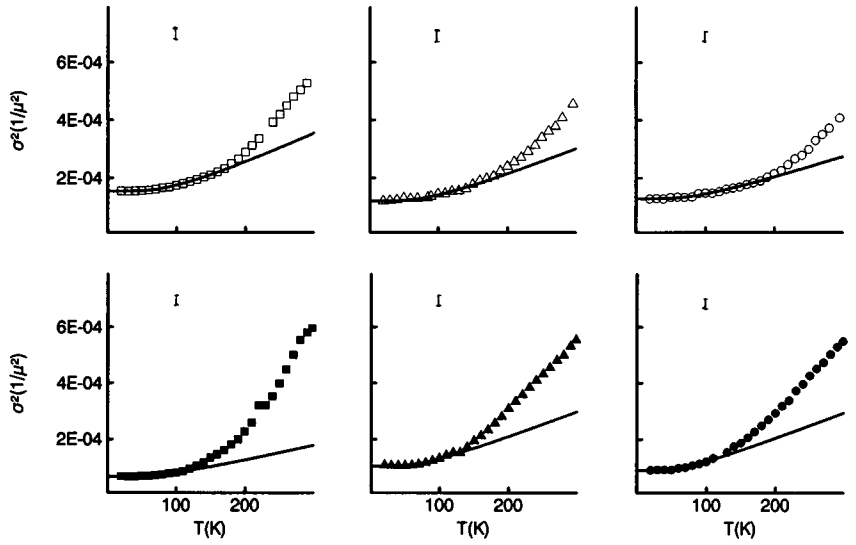

FIGURE 4 Temperature dependence of σ^2 values. Panels and symbols as in Fig.3. The continuous lines represent fittings of the data in the temperature range 20–160K (CO derivatives) and 20–110K (deoxy derivatives) in terms of Eq. 4. Typical error bars are reported.

behavior characterized by a rapid interconversion among different conformational substates of the biomolecule. We wish to stress, however, that our technique probes only motions coupled with the $\pi \rightarrow \pi^*$ electronic transition responsible for the Soret band and therefore internal protein motions localized in the proximity of the heme.

The data illustrated in Fig. 5, where the difference $\Delta\sigma^2$ between the experimental points and the continuous curves of Fig. 4 is plotted against temperature, show that the anharmonic contributions are higher for El-Mb than for the other two proteins. Furthermore, the data also indicate clear differences between the two ligation states. In particular, Fig. 5 shows that the anharmonic contributions are consistently larger in the deoxy than in the CO derivatives; this fact confirms the already suggested (Cupane et al., 1993) stabilizing effect of the liganded CO molecule on the dynamics of the heme pocket. Moreover, whereas for the CO derivatives the deviation of σ^2 from harmonic behavior starts at ~180 K, for the deoxy derivatives the same phenomenon occurs at a lower temperature (~110 K); this fact suggests that in the deoxy derivatives nonharmonic contributions to nuclear motions are already present below the glass transition of the external matrix. However, as clearly appears from Fig. 5, differences between El-Mb and Sw- (or Ho-) Mb are present only at temperatures greater than 210 K, where $\Delta\sigma^2$ values relative to El-Mb are larger than those relative to the other two proteins.

As already mentioned, we attribute the differences between the coupling constants relative to the deoxy derivatives of El-Mb on one side and Sw-Mb and Ho-Mb on the

TABLE 2 Values of the parameters obtained by fitting the σ_0 and ν_0 behavior in the temperature range 20–160 K (CO derivatives) and 20–110 K (deoxy derivatives) in terms of Eqs 3 and 4

	NS*	$\langle\nu\rangle$/cm^{-1}	R‡	$(\nu_{00} + C)$/cm^{-1}	σ_{in}/cm^{-1}§
El-Mb	0.2 ± 0.1	167 ± 15	1.01 ± 0.005	22,530 ± 2	—
Ho-Mb	0.4 ± 0.1	153 ± 10	1.02 ± 0.005	22,590 ± 2	—
Sw-Mb	0.5 ± 0.1¶	132 ± 10¶	1.02 ± 0.004	22,629 ± 2	—
El-MbCO	0.4 ± 0.1	190 ± 10	1.01 ± 0.005	23,404 ± 4	40 ± 30
Ho-MbCO	0.4 ± 0.1	179 ± 10	1.01 ± 0.005	23,553 ± 5	35 ± 20
Sw-MbCO	0.3 ± 0.2	180 ± 30	1.01 ± 0.002	23,567 ± 4	53 ± 38

* NS values were obtained under the assumption $R^2 \approx 1$.

‡ The R values reported are obtained by assuming the coupling with $N = 50$ low-frequency modes.

§ For the deoxy derivatives inhomogeneous broadening is taken into account by the parameter δ (see Fig. 6).

¶ NS and $\langle\nu\rangle$ values relative to Sw-Mb reported in this work are slightly different from the analogous ones (NS = 0.7 and $\langle\nu\rangle$ = 110) reported previously (Cupane et al., 1993). This is due to the fact that, in order to avoid the systematic misfits observed for deoxyhemoglobin and myoglobin at temperatures around 100 K and clearly evident in Fig. 4 of the paper by Cupane et al. 1993, fittings of the σ^2 thermal behavior have been restricted, for the deoxy derivatives, to the temperature range 20–110 K.

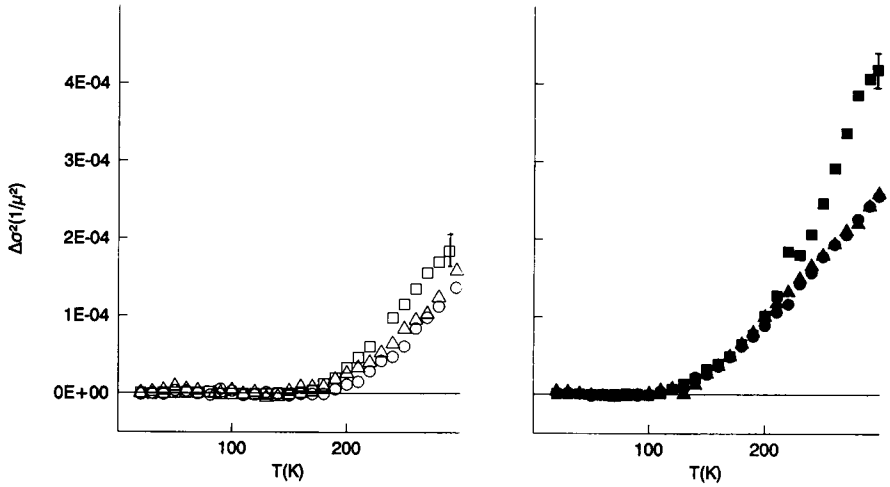

FIGURE 5 Differences between σ^2 values and extrapolated harmonic behavior. Left panel and open symbols refer to the CO derivatives, right panel and full symbols to the deoxy ones. Symbols as in Fig. 3; typical error bars are reported.

other to changes in heme doming. This interpretation finds further support in the data depicted in Fig. 6, where we report the values of parameters $Q_0\sqrt{b}$ and $\delta\sqrt{b}$ (see Eq. 3) as a function of temperature. In particular, the larger values of $Q_0\sqrt{b}$ found for El-Mb could be related to the presence of a linear term in Eq. 2; however, in view of the structural properties of El-Mb heme pocket, inferred from NMR investigations (Yu et al., 1990; Vyas et al., 1993), the assumption that the parameter b is the same for the three myoglobins investigated does not seem to be justified. Although a detailed interpretation of the data reported in Fig. 6 must await the solution of the three-dimensional structure of El-Mb, differences in the heme geometry in El-Mb with respect to the other two proteins are suggested by the behavior of $Q_0\sqrt{b}$. Furthermore, the low-temperature values of $\delta\sqrt{b}$ relative to El-Mb are consistently lower than those of Sw-Mb and Ho-Mb, in agreement with findings relative to σ^2 (Fig. 4, *bottom*). Moreover, the sharp increase in $\delta\sqrt{b}$ for El-Mb starting at ~230 K (Fig. 6) confirms the behavior of $\Delta\sigma^2$ reported in the right panel of Fig. 5 and indicates that the effect is not to be ascribed to artifacts arising from a compensation between $\Delta\sigma^2$ and $\delta\sqrt{b}$.

Flash photolysis

Also from the kinetic point of view, El-Mb displays peculiarities compared to Sw-Mb and Ho-Mb. The results described hereafter show that El-Mb is uncommon both for the number of kinetic components needed to describe its CO binding and for their thermal evolution, whereas Ho-Mb and Sw-Mb exhibit similar behavior (Table 3). We recall here that the kinetics of CO rebinding to Sw-Mb after flash photolysis can be described by a two-well model (Steinbach et al., 1991). The inner barrier, located at the heme iron, is characterized by a temperature-independent distribution of enthalpy barriers up to 160 K; above this temperature protein relaxation occurs and the barrier distribution shifts by about 10 kJ/mol to higher enthalpies. The outer barrier is that between the solvent and the heme pocket; at temperatures higher than 210 K ligand molecules can migrate through the fluctuating protein, and rebinding from the solvent (exponential in time since the barriers are averaged) can occur.

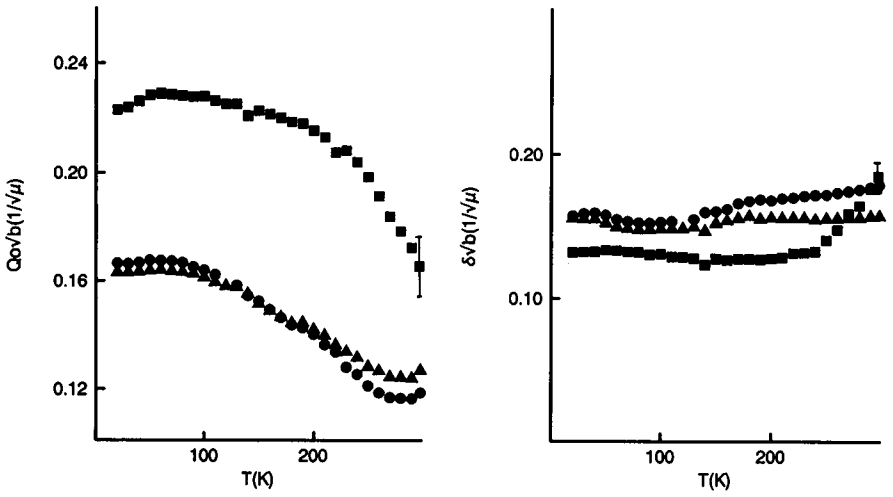

FIGURE 6 Temperature dependence of $Q_0\sqrt{b}$ (*left*) and of $\delta\sqrt{b}$ (*right*). Symbols as in Fig. 3. Error bars at high temperature are shown; at low temperature the errors decrease by more than a factor of two.

TABLE 3 Values of the fitting parameters for the five processes used to analyze the CO binding kinetics to El-Mb

	El-Mb Process I	El-Mb Process II	El-Mb Process III	El-Mb Process IV	El-Mb Process V	Ho-Mb	SW-Mb*	β-chains*
$\frac{H_{peak}}{(KJ/mol)}$	1.92 1.64 1.42	6.12 5.66 5.11	19.93 18.40‡ 16.58	29.81 28.88§ 26.85	33.65 ÷ 36.84¶	13.81 13.14 12.87	11.68 10.59 9.73	5.22 4.62 4.01
$\frac{FWHM}{(KJ/mol)}$	2.50	3.65	6.15	3.33‖	0	9.25	9.12	6.03
$\log\left(\frac{k_0}{s^{-1}}\right)$	8.56 8.46 8.35	8.81 7.87 7.01	11.06 10.95 10.02	10.78 10.03 9.82	9.30 9.18 9.01	9.41 9.11 8.92	9.33 9.01 8.81	9.74 9.63 9.52

The corresponding parameters for the pocket process of Ho- and Sw-Mb and those relative to the major low temperature kinetic component of the β hemoglobin chains are also given. The FWHM is not a fitting parameter and is computed from the $g(H)$ distribution as defined by H_{peak} and ψ (Eq. 7); their 67% confidence limits, computed from those of the fitting parameters, never exceed 13%.

* From Di Iorio et al., 1991.

‡ Between 40 and 180 K. See Fig. 8.

§ Between 120 and 180 K. See Fig. 8.

¶ Temperature dependent. See Fig. 8.

‖ Between 120 and 180 K. See Fig. 9.

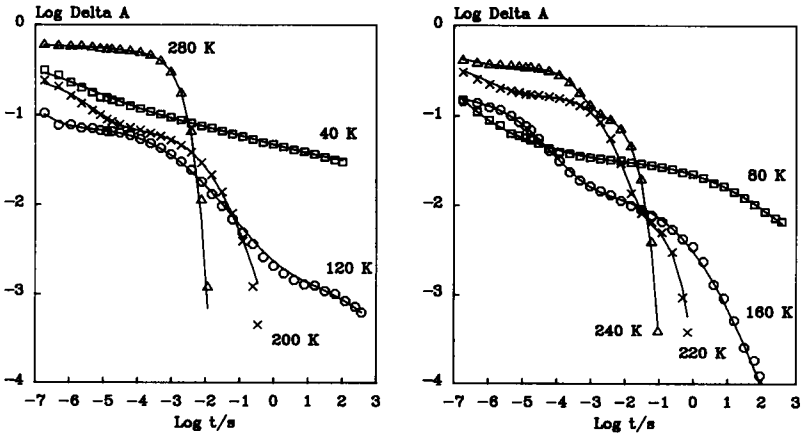

FIGURE 7 Time courses for CO recombination to El-Mb after photolysis at representative temperatures. Symbols refer to the experimental data while the continous curves have been obtained from the fitting parameters listed in Table 3 and reported in Figs. 8 and 9.

Representative kinetic traces for CO recombination to El-Mb in 75% glycerol, measured between 40 and 300 K, are illustrated in Fig. 7 along with the curves obtained by global fitting. The situation is more complicated than that found for Ho-Mb and Sw-Mb, since five distinct processes are needed to account for the kinetic traces over the whole temperature range; the values of the fitting parameters that characterize these processes are given in Figs. 8 and 9 and in Table 3.

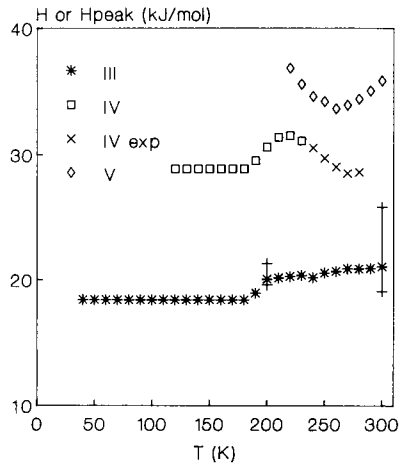

FIGURE 8 Temperature dependence of the activation enthalpy for processes III, IV, and V used to describe CO recombination to El-Mb after photolysis. While for processes III and V the activation enthalpy is distributed over the whole temperature range, for process IV this is the case only up to 230 K, above which temperature the kinetic process becomes exponential in time. The H_{peak} values for process III between 210 K and 290 K are affected by errors between those given for 200 K and 300 K.

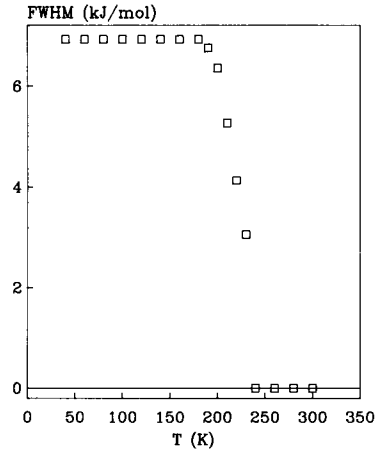

FIGURE 9 Temperature dependence of the width of the enthalpy distribution relative to process IV in the kinetics of CO binding to El-Mb. Above 230 K this kinetic step is exponential in time.

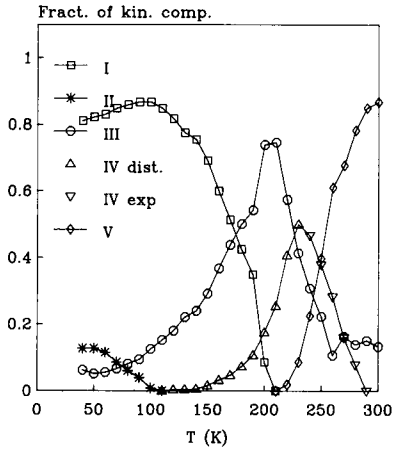

FIGURE 10 Temperature dependence of the amplitude of the five processes used to describe the kinetics of CO binding to El-Mb. The 67% confidence limits for the fractional amplitude of the various processes never exceed 2.2%. More details about the model used for the fitting of the data are given under Materials and Methods.

Process I displays a narrow $g(H)$ distribution (full width at half-maximum (FWHM) = 2.5 kJ/mol) peaked at only 1.6 kJ/mol (Table 3) and dominates at very low temperatures; however, its amplitude starts decreasing above ~100 K and drops to zero at ~210 K (Fig. 10). Very low peak activation enthalpies for CO rebinding have been reported for free heme (Alberding et al., 1976) and for cases in which photolysis dissociates both axial ligands of the iron (Huang et al., 1991; Di Iorio et al., 1993). However, two independent lines of evidence exclude the possibility that process I can be attributed to the photodissociation of the bond with the proximal histidine. The kinetic deoxy-carbonyl difference spectrum of El-Mb, reconstructed from the time zero amplitude of the kinetic traces recorded at 15 K as a function of wavelength (data not shown), does not show any feature that would indicate the rupture of the proximal bond. Furthermore, EPR spectra of reduced El-Mb-NO, recorded as a function of pH, show that the proximal bond is particularly strong in this protein since the typical nine-line hyperfine pattern, resulting from an overlap of the spectral contributions due to the nitrogens of the NO and of the proximal histidine (Bartnicki et al., 1983; Desideri et al., 1984; Trittelvitz et al., 1975), is very well resolved even at 77 K and still dominates at pH values as low as 4.3; moreover, the conversion to the characteristic triplet spectrum, typical of the penta-coordinated species (Desideri et al., 1984; Wailand and Olson, 1974), occurs only at pH 3.7, when most of the protein precipitates during sample preparation (data not shown). Having excluded the rupture of the proximal bond as being responsible, we attribute the low peak activation enthalpy of process I to CO recombination from the immediate vicinity of the heme iron, implying that after photolysis the ligand cannot travel a long distance before it rebinds. Structural requirements for this phenomenon to occur are a crowded heme pocket and/or a strong interaction of the bound ligand with distal residues. The presence of an additional phenylalanine in the heme pocket of El-Mb interacting with the bound ligand (Yu et al., 1990; Vyas et al., 1993) supports this hypothesis. A strong contribution of steric phenomena to the ligand binding behavior of El-Mb is also indicated by the thermal evolution of the CO binding kinetics and is consistent with the interpretation given hereafter for processes II through IV.

Process II, even though it is necessary to properly fit the kinetics of CO rebinding between 40 and 100 K, is moderately populated even at very low temperatures, and its amplitude drops to zero already at 110 K (Fig. 10). Based on this

experimental evidence, we attribute process II to CO recombination within protein molecules in which the photolysed ligand moves away from the immediate vicinity of the heme iron and populates a flashed-off state within the highly crowded heme pocket. This kind of "cage effect" is likely to occur only at very low temperatures, when only low-amplitude vibrational motions can take place, and therefore is bound to progressively disappear as temperature rises, as observed experimentally. The high entropic contribution to the free energy of ligand binding for process II (Table 3) probably reflects a considerable degree of disorder for the flashed-off state. In concomitance with the disappearence of process II, the amplitude of process I starts to decrease and process IV sets in. A plausible explanation for this complex behavior is provided by computational work (Loncharich and Brooks, 1990) showing, with molecular dynamics simulations of Sw-Mb, that soft dihedral transitions begin to occur at ~100 K. Based on this finding, we postulate that the onset of torsional motions, not necessarily of proper dihedral transitions, is responsible for the inversion in the thermal evolution of the amplitude of process I as well as for the disappearance of process II and for the appearance of process IV at ~110 K.

Only process III is populated in the whole 40–300 K temperature range, and therefore it can be identified as the "classical pocket process" already described in the literature for ligand binding to a number of heme proteins (Austin et al., 1975; Di Iorio et al., 1991; Di Iorio, 1992; Doster et al., 1982 and 1987; Stetzkowski et al., 1985). Below 180 K the peak activation enthalpy of process III is about 18 kJ/mol, considerably higher than the ~10 kJ/mol reported in the literature for the low-temperature pocket process in Sw-Mb or the ~13 kJ/mol found for Ho-Mb (Table 3). An increase in the values of H_{peak} is consistent with a more crowded heme crevice due to a stronger contribution of steric phenomena to the ligand binding enthalpy. Furthermore, process III has a pre-exponential of $\sim 10^{-11}$ s^{-1}, almost two orders of magnitude larger than in Sw-Mb and in Ho-Mb (Table 3); this is consistent with a reduction of the "effective volume" of the heme pocket that in turn brings about a lower entropic contribution to the free energy barrier for ligand recombination and leads to a higher pre-exponential (Braunstein et al., 1988; Frauenfelder and Wolynes, 1985). The peak position of the $g(H)$ relative to process III increases by ~2 kJ/mol between ~180 and ~200 K (Fig. 4), indicating protein "relaxation" (Agmon and Hopfield, 1983; Steinbach et al., 1991). The complexity of the kinetics and the time resolution of our traces do not enable an accurate determination of the H_{peak} above 200 K; for this reason we cannot give a precise estimate of the enthalpy increase upon relaxation. However, an upper limit for H_{peak} of process III of about 25–26 kJ/mol at 300 K can be determined, thus implying that the ΔH value linked to relaxation cannot be higher than ~8 kJ/mol. Process III, which accounts for only ~5% of the total absorbance change at 50 K, becomes more and more relevant as temperature increases up to 200–210 K, where it represents nearly 80% of the total signal difference between the fully ligated and the completely deoxy states. Above 210 K the amplitude of process III decreases again and around 260 K reaches a plateau at ~20%.

Another peculiarity in the kinetic behavior of El-Mb is the presence, above ~110 K, of process IV, which displays a particularly interesting thermal evolution. Below ~180 K the enthalpy distribution of this process is temperature independent and is characterized by an H_{peak} of ~28 kJ/mol and a FWHM of ~7 kJ/mol (Figs. 4 and 6). Conversely, above ~180 K both the width and the peak value of $g(H)$ are temperature dependent. The enthalpy distribution becomes progressively narrower as temperature rises, leading to an exponential binding above ~240 K. On the other hand, the peak enthalpy increases from ~28 kJ/mol at ~180 K to nearly 33 kJ/mol at ~220 K and then starts decreasing to reach again ~28 kJ/mol at ~260 K. Furthermore, the fractional amplitude of process IV is strongly influenced by temperature: it starts from zero below 110 K and increases to more than 0.5 at ~230 K to drop again to zero at ~290K. On the basis of these features we propose that process IV is related to a dynamic channel within the protein matrix through which the ligand can migrate, a ri-edition of the matrix process in the multibarrier model (Ansari et al., 1986; Austin et al., 1975; Di Iorio, 1992). The probability of the photolyzed CO molecule entering the channel is proportional to the frequency with which the "dynamic gate" opens and therefore rises with temperature. At ~180 K (the solvent glass transition temperature; Cordone et al., 1988) in addition to local motions of the residue(s) acting as a "channel gate," further fluctuations involving larger areas of the protein set in, and most likely because of protein relaxation, the free energy for ligand recombination increases. At ~220 K process V (solvent process, exponential in time) starts to be populated. The onset of ligand exchange between the protein interior and the surrounding medium indicates that the whole protein-solvent system has started fluctuating. Under these conditions the effect of local motions is, in our interpretation, reduced by fluctuations of the surrounding structure and therefore the activation enthalpy of process IV starts decreasing when process V sets in. Furthermore, above the glass transition the rate of interconversion between the "gate opened" and "gate closed" conformations increases progressively and therefore the width of the $g(H)$ distribution for process IV decreases up to a point (~240 K) at which the process becomes exponential. In light of this explanation it can be speculated that processes II and IV are associated with motions of the same group of atoms acting as a trap for the photolyzed ligand below 110 K and as a channel gate at higher temperatures.

Correlation between optical spectroscopy and flash photolysis data

The hierarchical organization of motions in proteins, already proposed by Ansari et al. (1985), is nicely evidenced by the results described in this paper. It is very fortunate that the

structural features of El-Mb are such that the sequence with which dynamic events evolve as temperature increases can be followed in detail; this can be attributed to a delicate interplay between proximal and steric phenomena that increase the "sensitivity" of the heme as a "probe" for detecting fluctuations, which are common (although to different extent) to all proteins. The convergence between optical spectroscopy and flash photolysis results makes it possible to suggest explanations for some of the observations that otherwise are not interpretable on the basis of either one of the experimental approaches alone.

In what follows we compare flash photolysis data with optical spectroscopy results concerning the deoxy derivatives; of course, we are aware of the fact that, at least at temperatures below 160 K, flash photolysis experiments monitor the kinetics of CO rebinding to protein molecules that have not relaxed to the equilibrium deoxy conformation.

Optical spectroscopy data show that for the deoxy derivatives of the three myoglobins investigated nonharmonic fluctuations start at about 110 K (Fig. 5, *right*). As mentioned above, torsional motions (Loncharich and Brooks, 1990) may be involved. On the other hand, flash photolysis data show that only for El-Mb is CO rebinding sensitive to these motions; in fact, at about 100 K process II disappears, the amplitude of process I starts to decrease and that of process III increases, and process IV sets in. In contrast, for Sw-Mb and Ho-Mb, a single process with a temperature-independent enthalpy distribution is sufficient to fit the kinetics of CO rebinding up to ~160 K (Steinbach et al., 1991; data in Table 3). This points out the subtle interplay between steric and dynamic effects that are relevant to protein function: the nonharmonic fluctuations starting at ~110 K (that are a prerequisite for substate interconversion) likely constitute, following Frauenfelder (1985), "functionally important motions" (FIMs) for El-Mb, due to the crowded structure of its heme pocket, while the same motions are likely to be "biologically unimportant motions" (BUMs) for Sw- or Ho-Mb, in view of the more open structure of their heme pockets.

Optical spectroscopy data show also that at temperatures higher than ~200 K El-Mb starts behaving differently from both Sw- and Ho-Mb. This is consistently evidenced by the thermal behavior of $\Delta\sigma^2$ (Fig. 5, *left*), ν_0 (Fig. 3, *bottom*), and $\delta\sqrt{b}$ (Fig. 6, *right*) that point out larger-amplitude motions in El-Mb with respect to the other two myoglobins that we attribute to an increased "flexibility" of this protein. The temperature dependence of the spectral parameters relative to El-Mb well correlates with the onset of the solvent process (V) in the CO rebinding kinetics (together with the concomitant decrease of the amplitude of process III; Fig. 10) and with the thermal behavior of the activation enthalpy for process IV (Figs. 8 and 9). The increased "flexibility" of El-Mb with respect to Sw- and Ho-Mb is also supported by the correlation between the low-temperature values of $\delta\sqrt{b}$ (Figs. 3 and 6) and the width of the activation enthalpies for CO rebinding (Table 3). The low-temperature values of $\delta\sqrt{b}$ relative to El-Mb are smaller than those of Sw-Mb and Ho-Mb (Figs. 4 and 5); on the other hand, the width of the activation enthalpy distributions for CO recombination to El-Mb are well below the ~9 kJ/mol observed for the pocket process of Sw-Mb and of Ho-Mb (Table 3). In particular, the $g(H)$ for process III, identified as the "classical pocket process," has a width of about 6 kJ/mol, the same reported for the β human hemoglobin chains (Table 3). This correlation confirms previous studies from our groups (Di Iorio et al., 1991), in which it was shown that narrow enthalpy distributions for ligand binding correspond to low values of the parameters that determine the width of optical bands and which showed an inverse relation between the width of the $g(H)$ and of the spectral bands on one side and the "flexibility" of the protein on the other.

We are indebted to Prof. Arthur Schweiger and Mr. Walter Lämmler, from the Laboratory of Physical Chemistry of the ETH Zurich, for performing the EPR measurements, to Prof. R.W. Noble for useful discussions, to Prof. G. N. La Mar for providing the paper by Vyas et al. prior to its publication and to Mr. G. Lapis, Mr. A. Lehman, and Mr. M. Quartaro for technical help. We also wish to express our gratitude to the pathology department of the Veterinary Clinic of the Canton Zurich for providing heart and skeletal muscle from two deceased elephants from local zoological gardens.

This work has been supported by grants from the Italian "Ministero per l'Università e per la Ricerca Scientifica e Tecnologica" and from the the Swiss National Science Foundation grant 31.9432.88 as well as by the ETH special credit 03586/41-1080.5. General indirect support from the Sicilian CRRNSM is also gratefully acknowledged.

REFERENCES

Agmon, N., and J. J. Hopfield. 1983. CO binding to heme proteins: a model for barrier height distributions and slow conformational changes. *J. Chem. Phys.* 79:2042–2053.

Alberding, N., R. H. Austin, S. C. Shirley, L. Eisenstein, H. Frauenfelder, I. C., Gunsalus, and T. M. Nordlund. 1976. Dynamics of carbon monoxide binding to protoheme. *J. Chem. Phys.* 65:4701–4711.

Ansari, A., E. E. Di Iorio, D. D. Dlott, H. Frauenfelder, I. E. T. Iben, P. Langer, H. Roder, T. B. Sauke, and E. Shyamsunder. 1986. Ligand binding to heme proteins: relevance of low-temperature data. *Biochemistry.* 25:3139–3146.

Ansari, A., J. Berendzen, S. F. Bowne, H. Frauenfelder, I. E. T. Iben, T. B. Sauke, E. Shyamsunder, and R. D. Young. 1985. Protein states and proteinquakes. *Proc. Natl. Acad. Sci. USA.* 85:5000–5004.

Asher, S. A., M. L. Adams, and T. M. Schuster. 1981. Resonance raman and absorption spectroscopic detection of distal histidine-fluoride interaction in human methemoglobin-dluoride and sperm whale metmyoglobin fluoride: measurements. *Biochemistry.* 20:3339–3346.

Austin, R. H., K. W. Beeson, L. Eisenstein, H. Frauenfelder, and I. C. Gunsalus. 1975. Dynamics of ligand binding to myoglobin. *Biochemistry.* 14:5355–5373.

Bangcharoenpaurpong, O., K. T. Schomacker, and P. M. Champion. 1984. A resonance raman investigation of myoglobin and hemoglobin. *J. Am. Chem. Soc.* 106:5688–5698.

Bartnicki, D. E., H. Mizukami, and A. E. Romero-Herrera. 1983. Interaction of ligands with the distal glutamine in elephant myoglobin. *J. Biol. Chem.* 258:1599–1602.

Bevington, P. R. 1969. Data Reduction and Error Analysis for the Physical Sciences. McGraw-Hill, New York. 242–245.

Braunstein, D., A. Ansari, J. Berendzen, B. R. Cowen, K. D. Egeberg, H. Frauenfelder, M. K. Hong, P. Ormos, T. B. Sauke, R. Scholl, A. Schulte, S. G. Sligar, B. A. Springer, P. J. Steinbach, and R. D. Young. 1988. Ligand binding to synthetic mutant myoglobin (His E7 → Gly): role of the distal histidine. *Proc. Natl. Acad. Sci. USA.* 85:8497–8501.

Cordone, L., A. Cupane, M. Leone, and E. Vitrano. 1986. Optical absorption spectra of deoxy- and oxyhemoglobin in the temperature range 300–20

K. Relation with protein dynamics. *Biophys. Chem.* 24:259–275.

Cordone, L., A. Cupane, M. Leone, E. Vitrano, and D. Bulone. 1988. Interaction between external medium and heme pocket in myoglobin probed by low temperature optical spectroscopy. *J. Mol. Biol.* 199:213–218.

Cupane, A., M. Leone, E. Vitrano, and L. Cordone. 1988. Structural and dynamic properties of the heme pocket in myoglobin probed by optical spectroscopy. *Biopolymers.* 27:1977–1997.

Cupane, A., M. Leone, and E. Vitrano. 1993. Protein dynamics: conformational disorder, vibrational coupling and anharmonicity in deoxyhemoglobin and myoglobin. *Eur. Biophys. J.* 21:385–391.

Dene, H., M. Goodman, and A. E. Romero-Herrera. 1980. The amino acid sequence of elephant (*Elephas maximus*) myoglobin and the phylogeny of Proboscidea. *Proc. R. Soc. Lond.* B207:111–127.

Desideri, A., U. T. Meier, K. H. Winterhalter, and E. E. Di Iorio. 1984. Electron paramagnetic resonance properties of liver fluke (*Dicrocoelium dendriticum*) nitrosyl hemoglobin. *FEBS Lett.* 166:378–380.

Di Iorio, E. E. 1981. Preparation of derivatives of ferrous and ferric hemoglobin. *Methods Enzymol.* 76:57–72.

Di Iorio, E. E. 1992. Protein dynamics. An overview on flash-photolysis over broad temperature ranges. *FEBS Lett.* 307:14–19.

Di Iorio, E. E., K. H. Winterhalter, and G. M. Giacometti. 1987. Isocyanide binding kinetics to monomeric hemoproteins. A study on the ligand partition between solvent and heme pocket. *Biophys. J.* 51:357–362.

Di Iorio, E. E., U. R. Hiltpold, D. Filipovic, K. H. Winterhalter, E. Gratton, E. Vitrano, A. Cupane, M. Leone, and L. Cordone. 1991. Protein dynamics. Comparative investigation on heme-proteins with different physiological roles. *Biophys. J.* 59:742–754.

Di Iorio, E. E., W. Yu, C. Calonder, K. H. Winterhalter, G. De Sanctis, G. Falcioni, F. Ascoli, B. Giardina, and M. Brunori. 1993. Protein dynamics in minimyoglobin: is the central core of myoglobin the conformational domain? *Proc. Natl. Acad. Sci. USA.* 90:2025–2029.

Di Pace, A., A. Cupane, M. Leone, E. Vitrano, and L. Cordone. 1992. Protein dynamics: vibrational coupling, spectral broadening mechanisms and anharmonicity effects in carbonmonoxy heme proteins studied by the temperature dependence of the Soret band lineshape. *Biophys. J.* 63:475–484.

Doster, W., D. Beece, S. F. Bowne, E. E. Di Iorio, L. Eisenstein, H. Frauenfelder, L. Reinisch, E. Shyamsunder, K. H. Winterhalter, and K. T. Yue. 1982. Control and pH dependence of ligand binding to heme proteins. *Biochemistry.* 21:4832–4839.

Doster, W., S. F. Bowne, H. Frauenfelder, L. Reinisch, and E. Shyamsunder. 1987. Recombination of carbon monoxide ferrous horseradish peroxidase types A and C. *J. Mol. Biol.* 194:299–312.

Doster, W., S. Cusack, and W. Petry. 1989. Dynamical transition of myoglobin revealed by inelastic neutron scattering. *Nature (Lond.).* 337: 754–756.

Frauenfelder, H. 1985. Ligand binding and protein dynamics. In Structure and Motion: Membranes, Nucleic Acids and Proteins. E. Clementi, G. Corongiu, M. H. Sarma, and R. H. Sarma, editors. Adenine Press, New York. 205–217.

Frauenfelder, H., and P. G. Wolynes. 1985. Rate theories and puzzles of hemeprotein kinetics. *Science (Washington DC).* 229:337–345.

Frauenfelder, H., F. Parak, and R. D. Young. 1988. Conformational substates in proteins. *Annu. Rev. Biophys. Chem.* 17:451–479.

Huang, Y., M. C. Marden, J. C. Lambry, M. P. Fontaine-Aupart, R. Pansu, J. L. Martin, and C. Poyart. 1991. Photolysis of the histidine-heme-CO complex. *J. Am. Chem. Soc.* 113:9141–9144.

Kerr, E. A., N. T. Yu, D. E. Bartniki, and H. Mizukami. 1985. Resonance Raman studies of carbon monoxide and oxygen binding to elephant myoglobin [distal His(E7)-Gln]. *J. Biol. Chem.* 260:8360–8365.

Krupyanskii, Y. F., V. I. Goldanskii, G. U. Nienhaus, and F. Parak. 1990. Dynamics of protein-water systems revealed by Rayleigh scattering of Mössbauer radiation (RSMR). *Hyperfine Interactions.* 53:59–74.

Leone, M., A. Cupane, E. Vitrano, and L. Cordone. 1987. Dynamic properties of oxy- and carbonmonoxy-hemoglobin probed by optical spectroscopy in the temperature range of 300–20 K. *Biopolymers.* 26: 1769–1779.

Leone, M., A. Cupane, E. Vitrano, and L. Cordone. 1992. Strong vibronic coupling in heme proteins. *Biophys. Chem.* 42:111–115.

Loncharich, R. J., and B. R. Brooks. 1990. Temperature dependence of dynamics of hydrated myoglobin. Comparison of force field calculations with neutron scattering data. *J. Mol. Biol.* 215:439–455.

Marquardt, D. W. 1963. An algorithm for least-squares estimation of nonlinear parameters. *J. Soc. Ind. Appl. Math.* 11:431–441.

Mims, M. P., A. G. Porras, J. S. Olson, R. W. Noble, and J. A. Peterson. 1983. Ligand binding to heme proteins: an evaluation of distal effects. *J. Biol. Chem.* 158:14219–14232.

Parak, F. 1989. Structural distributions, fluctuations and conformational changes in prroteins investigated by Mössbauer spectroscopy and X-ray structure analysis. *NATO Adv. Study Inst. Ser. Ser. A. Life Sci.* 178: 197–221.

Richter, C., and E. E. Di Iorio. 1991. Analysis of the membrane-bound cytochrome P-450 system by the flash photolysis technique. Frontiers in Biotrasformation. Vol. 5. K. Ruckpaul and H. Rein, editors. Akademie Verlag, Berlin. 72–93.

Romero-Herrera, A. E., M. Goodman, H. Dene, D. E. Bartnicki, and H. Mizukami. 1981. An exceptional amino acid replacement on the distal side of the iron atom in proboscidean myoglobins. *J. Mol. Evol.* 17: 140–147.

Schomacker, K. T., and P. M. Champion. 1989. Investigations of the temperature dependence of resonance Raman cross sections: applications to hemeproteins. *J. Chem. Phys.* 90:5982–5993.

Srajer, V., K. T. Schomacker, and P. M. Champion. 1986. Spectral broadening in biomolecules. *Phys. Rev. Lett.* 57:1267–1270.

Srajer, V., P. M. Champion. 1991. Investigations of optical line shapes and kinetic hole burning in myoglobin. *Biochemistry.* 30:7390–7402.

Smith, J., K. Kuczera, and M. Karplus. 1990. Dynamics of myoglobin: comparison of simulation results with neutron scattering spectra. *Proc. Natl. Acad. Sci. USA.* 87:1601–1605.

Steinbach, P. J., A. Ansari, J. Berendzen, D. Braunstein, K. Chu, B. R. Cowen, D. Ehrenstein, H. Frauenfelder, J. B. Johnson, D. C. Lamb, S. Luck, J. R. Mourant, G. U. Nienhaus, P. Ormos, R. Philipp, R. Scholl, A. Xie, and R. D. Young. 1991. Ligand binding to heme proteins: connection between dynamics and function. *Biochemistry.* 30:3988–4001.

Stetzkowski, F., R. Banergjee, M. C. Marden, D. K. Beece, S. F. Bowne, W. Doster, L. Eisenstein, H. Frauenfelder, L. Reinisch, E. Shyamsunder, and C. Jung. 1985. Dynamics of dioxygen and carbon monoxide binding to soybean leghemoglobin. *J. Biol. Chem.* 260:8803–8809.

Trittelvitz, E., K. Gersonde, and K. H. Winterhalter. 1975. Electron-spin resonance of nitrosyl haemoglobins: normal α and β chains and mutants Hb M Iwate and Hb Zurich. *Eur. J. Biochem.* 51:33–42.

Tsubaki, M., R. B. Srivastava, and N. Yu. 1982. Resonance raman investigation of carbon monoxide bonding in (carbonmonoxy) hemoglobin and -myoglobin: detection of Fe-CO stretching and Fe-C-O bending vibrations and influences of the quaternary structure change. *Biochemistry.* 21:1132–1140.

Vyas, K., K. Rajarathnam, L. P. Yu, S. D. Emerson, G. N. La Mar, R. Krishnamoorhi, and H. Mizukami. 1993. ^{1}H NMR investigation of the heme cavity of elephant (E7 Gln) metMbCN: evidence for a B-helix phenylalanine interaction with bound ligand. *J. Biol. Chem.* 268:14826–14835.

Wailand, B. B., and L. W. Olson. 1974. Spectroscopic studies and bonding model for nitric oxide complexes of iron porphyrins. *J. Am. Chem. Soc.* 96:6037–6041.

Winkler, H., M. Franke, A. X. Trautwein, and F. Parak. 1990. Recombination studies of photodissociated MbCO by Mössbauer spectroscopy at low temperatures. *Hyperfine Interactions.* 58:2405–2412.

Wittenberg, J. B., and B. A. Wittenberg. 1981. Preparation of myoglobins. *Methods Enzymol.* 76:29–54.

Young, R. D., and S. F. Bowne. 1984. Conformational substates and barrier height distributions in ligand binding to heme proteins. *J. Chem. Phys.* 81:3730–3737.

Yu, L. P., G. N. La Mar, and H. Mizukami. 1990. Rearrangement of the distal pocket accompanying E7 His $\rightarrow$ Gln substitution in elephant carbonmonoxy- and oxymyoglobin: ^{1}H NMR identification of a new aromatic residue in the heme pocket. *Biochemistry.* 29:2578–2585.